TABLE II. Results compared with calculated values for molecular and atomic hydrogen.

Energy (keV)	Measured attenuation (cm²/g)	Calculated attenuation[a] Atomic (cm²/g)	Calculated attenuation[a] Molecular[b] (cm²/g)
25.0	0.3640 ± 0.0035	0.3629	0.3665
22.1	0.3711 ± 0.0018	0.3666	0.3711
14.4	0.3869 ± 0.0021	0.3773	0.3878
6.46	$0.4401^{+0.0017}_{-0.0018}$	0.3997	0.4503

[a]Interpolated from Ref. 2 with the inclusion of the photoelectric effect.

[b]Includes the molecular photoelectric effect correction described in Ref. 4.

included in quadrature with statistical uncertainties in determining the uncertainty in the attenuation coefficient.

At the three higher energies (25.0, 22.1, and 14.4 keV), our results agree very well with the calculations[2] based on the form factors of Bentley and Stewart.[3] Agreement is to better than 1 standard deviation (< 1%) at all three energies (see Table II). We note that at these energies the attenuation is predominantly due to scattering.

At our lowest energy (6.46 keV), we show our greatest disagreement with the theory [(2.2 ± 0.4)%]. (At this energy, the photoelectric effect accounts for 4% of the attenuation. We include the molecular correction[4] for the photoelectric effect in the theoretical value.) Since the measured value is smaller than the theoretical value, this may indicate that the molecular corrections contained

in the theory (at this energy) are too large. The magnitude of the molecular effect at this energy, however, is 12% and hence considerably larger than at any of the higher energies. Our results at this energy differ from the atomic values[2] by 25 standard deviations. If this difference were due to impurities, it would mean the presence of roughly 300 ppm of nitrogenlike gases. We are confident that such a large amount would not have escaped undetected. Hence, we conclude from these results that molecular considerations are important in accurately describing attenuation in H_2 gas. From Table II, it is seen that our conclusion regarding the existence of the molecular effects is also supported by the results at 14.4 and 22.1 keV.

We would like to thank Professor Leon M. Lederman for suggesting this experiment, and for his continuing interest.

[1]J. H. Hubbell, At. Data 3, 241 (1971).
[2]J. H. Hubbell et al., J. Phys. Chem. Ref. Data 4, 471 (1975).
[3]J. J. Bentley and R. F. Stewart, J. Chem. Phys. 62, 875 (1975).
[4]J. W. Cooper, Phys. Rev. A 9, 2236 (1974).
[5]J. T. Routti and S. G. Prussin, Nucl. Instrum. Methods 72, 125 (1969).

Parametric Excitation of Electrostatic Ion Cyclotron Waves in a Multi–Ion-Species Plasma*

M. Ono and M. Porkolab†
Plasma Physics Laboratory, Princeton University, Princeton, New Jersey 08540

and

R. P. H. Chang
Bell Laboratories, Murray Hill, New Jersey 07974
(Received 23 February 1977)

Parametric excitation of the electrostatic ion cyclotron waves in a multi–ion-species plasma is observed. The modes are excited when the pump frequency is near the sum of the ion cyclotron frequencies. The dispersion relation and the threshold for excitation are measured.

Although predicted by theory, up until now, to our knowledge, no experimental verification of the parametric instability near the ion cyclotron

frequency has been reported.[1] In this Letter we wish to report experimental observation of the electrostatic-ion-cyclotron-wave parametric in-

stability in a two–ion-species plasma. Such an instability may occur, for example, during radio-frequency heating near the ion cyclotron frequency of a deuterium-tritium fusion reactor plasma.[1] Since parametric instabilities may produce anomalous absorption of the incident microwave power, it is of importance to understand under what conditions they may occur.

The present instability is induced mainly by the relative polarization drift between the ions of different species. Although the electron drift is comparable in strength to ion drift, theory shows that for hot electrons its contribution to driving the instability is negligible.[1] The resulting decay

waves propagate in the direction of the pump electric field, perpendicularly to the external magnetic field. In a two–ion-species plasma, the dispersion relation of electrostatic waves predicts two propagation modes, one above each ion cyclotron frequency. The real part of this dispersion relation in a plasma with hot electrons and cold ions is given by the following expression:

$$1 + \frac{1}{k^2 \lambda_{De}^2} - \frac{\omega_{p1}^2}{\omega^2 - \Omega_1^2} - \frac{\omega_{p2}^2}{\omega^2 - \Omega_2^2} = 0; \qquad (1a)$$

for finite ion temperature, the real part of the hot-plasma dispersion relation is given by the following expression:

$$1 + \frac{1}{k^2 \lambda_{De}^2} - \frac{1}{k^2} \sum_{\sigma=1,2} \frac{\omega_{p\sigma}^2 m_\sigma}{T_\sigma} \sum_{n=1}^{\infty} I_n \left(\frac{k_\perp^2 T_\sigma}{m_\sigma \Omega_\sigma^2} \right) \exp \left(- \frac{k_\perp^2 T_\sigma}{m_\sigma \Omega_\sigma^2} \right) \frac{2 n^2 \Omega_\sigma^2}{\omega^2 - n^2 \Omega_\sigma^2} = 0. \qquad (1b)$$

Here ω and k are the wave frequency and wave number, Ω_1 and Ω_2 are the ion cyclotron frequencies of each ion species, ω_{p1} and ω_{p2} are the ion plasma frequencies, λ_{De} is the electron Debye length, $T_1 = T_2$ is the ion temperature, and I_n is the modified Bessel's function of the first kind. In contrast to the well-known Buchsbaum ion-ion hybrid modes (which occur in a cold electron plasma),[2] we shall call the present modes "kinetic ion-ion hybrid modes" (since these occur in a hot electron plasma). We note that for a single–ion-species plasma, these modes would reduce to the usual electrostatic ion cyclotron waves.[3,4] Furthermore, decay into these two modes may occur for a large range of plasma parameters. Writing the cold-ion dispersion relation for each of the decay waves, $\omega_1(k)$ and $\omega_2(k)$, and using the selection rules $\omega_0 = \omega_1 + \omega_2$ and $k_0 = k_1 + k_2 = 0$ (so that $k_1 = -k_2$), we obtain the following relation for the lower sideband, $\omega_2(k_2)$:

$$(\omega_2^2 - \Omega_1^2)[(\omega_0 - \omega_2)^2 - \Omega_1^2] - (N_1 m_2 / N_2 m_1)(\omega_2^2 - \Omega_2^2)[\Omega_2^2 - (\omega_0 - \omega_2)^2] = 0. \qquad (2)$$

Here, N_1 and N_2 are the relative ion concentrations, and m_1 and m_2 are the masses of the two ion species with m_2 being the mass of lighter ion species. We note that for a given pump frequency and ion species, the decay wave frequency depends only upon the relative ion concentration ratio and the magnetic field strength, and is independent of the wave number. Hence, it will be relatively easy to check experimentally the selection rules through Eq. (2).

The threshold for exciting this instability in a finite-length system is given by the following expression[5,6]:

$$\gamma_0^2 = V_1 V_2 \left[\frac{\pi^2}{4L^2} + \frac{1}{4} \left(\frac{\Gamma_1}{V_1} + \frac{\Gamma_2}{V_2} \right)^2 \right], \qquad (3)$$

where

$$\gamma_0^2 = \frac{k^2 U^2 |\chi_1 - \chi_2|^2}{4(\partial \epsilon / \partial \omega_1) \partial \epsilon / \partial \omega_2}$$

is the growth rate in a uniform plasma.[1] Here L is the size of plasma column which is usually ~ 4–5 cm, $V_{1,2}$ are the group velocities of the two

decay waves, $\Gamma_{1,2}$ are their damping rates, $\chi_1 = \chi(\omega)$ and $\chi_2 = \chi(\omega - \omega_0)$ are the ion susceptibilities of the lighter-mass ion species, and $U \cong cE \omega_0 \Omega_2 / B(\omega_0^2 - \Omega_2^2)$ is the relative polarization drift of ions (where we assumed $\Omega_1 \ll \Omega_2$).[1]

The experiments were performed in the Princeton University L-4 device. A schematic of the experimental apparatus is shown in Fig. 1. A hot electron plasma was produced by a tungsten filament source.[7] The range of experimental parameters were as follows: the magnetic field, $B_0 \lesssim 4.2$ kG; the plasma density, $N_0 = \sim 10^9$–10^{10} cm^{-3}; the temperatures, $T_e = 3$–5 eV and $T_i < 0.1$ eV; and neutral gas filling pressure in the experimental region, $P \cong 1.0 \times 10^{-4}$ Torr. A plasma with desired ion concentration ratio was produced by properly adjusting the inflow of neutral gases 1 and 2. The relative ion concentration was measured by combined spectroscopic and Langmuir-probe techniques. The external rf oscillator was coupled to the rf structure through an impedance-matching network. The pump electric field and
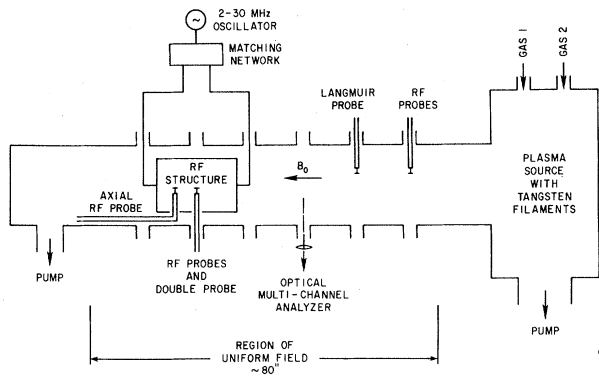
FIG. 1. Simplified schematic of the experimental set-up.

the resulting decay waves which propagate in the central region of the structure were investigated by radially and axially movable rf probes and also with calibrated ceramic-insulated double probes.

The rf induction coil structure was built of copper coils embedded in a ceramic insulator and was electrostatically shielded from the plasma by a Faraday shield. The structure was aligned parallel to the magnetic field lines so that the induced electric field was perpendicular to the external dc magnetic field. We have designed the shape of the coil so that the electric field induced by it was uniform in the central region of the plasma column with effective parallel wavelength of 15 cm. Because of the low plasma density, the rf electric field generated inside the plasma was essentially the vacuum field, and could be calculated directly from Maxwell's equations. The Faraday shield isolated the plasma from the electrostatic field produced by the inductive potential drop along the coil. In order to determine the exact nature of the pump electric field, we have searched for short-wavelength electrostatic waves at the pump frequency, using interferometric techniques. However, our search proved negative, and we concluded that the pump electric field could be correctly described in the dipole approximation, namely $k_{0\perp} = 0$.

As the pump power was increased above a certain threshold level, we observed a sudden onset of parametric decay. A typical decay frequency spectrum obtained in a helium-neon plasma is shown in Fig. 2(a). (We note that similar decay waves were also observed in helium-argon or helium-krypton plasmas.) The subsequent data presented in this paper were obtained in a helium-
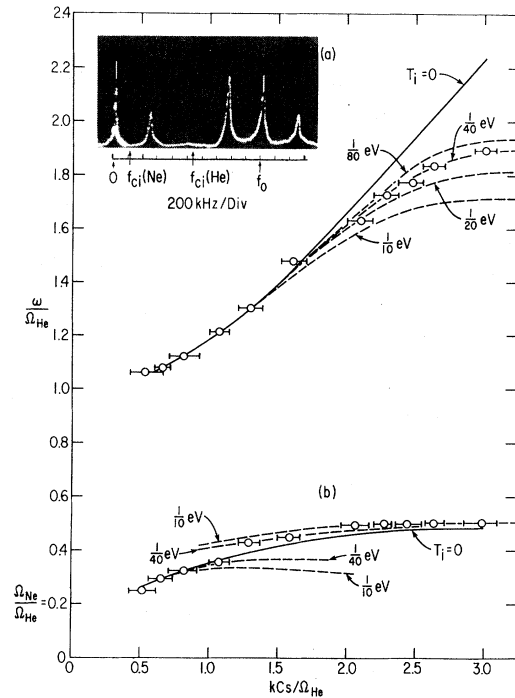

FIG. 2. (a) Parametric decay spectrum. f_{ci}(He) and f_{ci}(Ne) are the helium and neon ion cyclotron frequencies. ($B_0 = 2.9$ kG, $f_0 = 2$ MHz, He:Ne = 4:6). (b) Dispersion curve of kinetic ion-ion hybrid mode. Solid and dashed curves, theory. (He:Ne = 4:6, Cs is the helium acoustic speed.) Circles are experimentally measured values.

neon plasma. As shown in Fig. 2(a) the decay frequencies were observed to occur above each ion cyclotron frequency, and varied with the magnetic field and relative ion concentration ratio. From the variation of the decay frequencies with magnetic field strength, the dependence of the frequencies upon ion concentration ratio, and wavelength measurements with interferometric techniques, the decay waves were identified to be the kinetic ion-ion hybrid waves.

The theoretical dispersion curves for the two kinetic ion-ion hybrid modes, in a 4:6 He-Ne ion mixture, as predicted by Eq. (1), is shown by the solid curves in Fig. 2. In the same figure, the circles show the experimentally measured values of $\omega(k)$, as determined by interferometric measurements of the wave numbers of the decay waves. We believe that this is the first experimental observation of the kinetic ion-ion hybrid modes. We see good agreement between the experimentally measured values and cold-plasma theory, except near the harmonics of the ion cy-
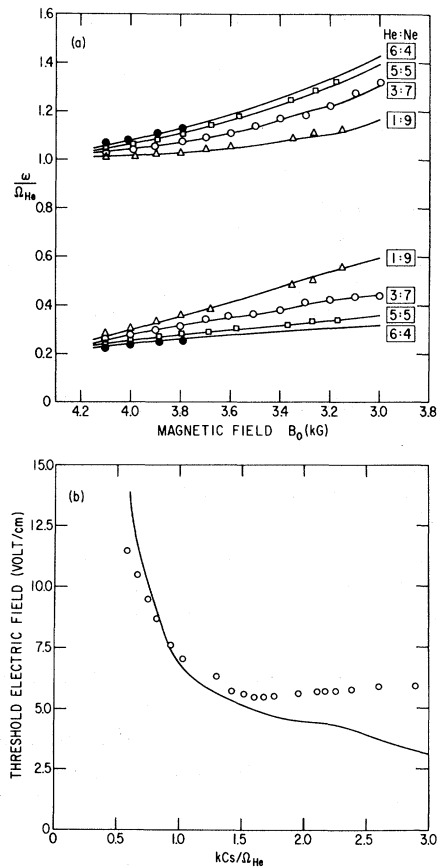
FIG. 3. (a) Decay wave frequency vs magnetic field for various ion concentration ratios. Circles and dots are the experimentally measured values, and the solid lines correspond to theory. $f_0 = 2$ MHz. (b) Threshold value of pump electric field vs wave number of decay waves. Solid curve corresponds to theory (He:Ne = 4:6).

clotron frequencies. In order to explain this deviation from the cold-ion-plasma theory, we have numerically calculated the hot-plasma electrostatic wave dispersion relation as shown by Eq. (1b), including finite-ion-Larmor-radius effects. In Fig. 2, we show such theoretical plots (indicated as dotted lines) for different ion temperatures which may be expected in our device. We see that the best agreement between theory and experiment is obtained by assuming $T_i \simeq \frac{1}{40}$ eV (or T_i approximately equal to room temperature). We note that in two-ion-species plasmas the gap in the dispersion curves near the second ion cyclotron harmonic frequency is considerably enhanced by the finite-ion-Larmor-radius effects (especially for the lighter species). Thus, these experiments provide an interesting technique to esti-

mate the low ion temperatures that characterize plasma devices such as ours.

In Fig. 3(a), we have plotted the experimentally observed decay frequencies, normalized by a unit of helium ion cyclotron frequency, for various ratios of ion concentration as a function of magnetic field. The solid lines are the theoretical curves. We see that the experimentally observed values are again in good agreement with the theoretical curves.

In Fig. 3(b), we show the experimentally observed threshold values of pump electric field E as a function of the normalized wave number, kCs/Ω_{He}. The theoretical threshold curve for the decay instability was calculated from Eq. (3) with use of electron Landau damping, ion-ion collisions among the different ion species, and ion-neutral collisions in the imaginary parts, and finite-ion-Larmor-radius effects in the real part of the plasma dielectric constant. For our experimental parameters, ion Landau damping and ion cyclotron damping are negligible. The ion-ion collisions among different ion species become significant for relatively high-density cold-ion plasma. For our experimental parameters, their contribution is comparable to that of the ion-neutral collisions, and hence, were appropriately included in the threshold calculations. The electron Landau damping is estimated from the measured parallel wavelength of the decay waves, which is typically 4 to 5 cm. The comparison of the experimentally measured values (using the calibrated rf probe) with the theoretically obtained values shows good agreement, well within the experimental uncertainty which is typically a factor of 2. We note that the systematic deviation between theory and experiment for $kCs/\Omega_{\text{He}} \geq 2$ may be due to viscous ion damping,[8] which was not included in our calculations.

In conclusion, we have observed two-ion-species parametric instabilities near the ion cyclotron frequency. The measured dispersion relationship shows a good agreement with the theoretical prediction for the kinetic ion-ion hybrid mode. The dependence of wave-matching conditions upon ion concentration ratio and magnetic field are in good quantitative agreement. The observed thresholds are also found to be consistent with the theory. The saturation mechanism and the associated plasma heating are now under detailed study.

We thank P. Bellan, L. Johnson, and E. Hinnov for helpful discussions, and J. Johnson, J. Taylor, A. Sivo, and R. McWilliams for technical as-

sistance.

---

†Present address: Physics Department, Massachusetts Institute of Technology, Cambridge, Mass. 02139.

[1] J. L. Sperling and F. W. Perkins, Phys. Fluids 17, 1857 (1974).
[2] S. J. Bucksbaum, Phys. Fluids 3, 418 (1960).
[3] W. E. Drummond and M. N. Rosenbluth, Phys. Fluids 5, 1507 (1962).
[4] E. R. Ault and H. Ikezi, Phys. Fluids 13, 2874 (1970).
[5] M. Porkolab and R. P. H. Chang, Phys. Fluids 13, 2054 (1970); also D. Pesme, G. Laval, and R. Pellat, Phys. Rev. Lett. 31, 203 (1973).
[6] The finite-length effect becomes important near the ion cyclotron frequency.
[7] R. Limpaecher and K. R. Mackenzie, Rev. Sci. Instrum. 44, 726 (1973).
[8] M. Porkolab, Phys. Fluids 11, 834 (1968).

Theory of Strongly Turbulent Two-Dimensional Convection of Low-Pressure Plasma*

R. N. Sudan and M. Keskinen

Laboratory of Plasma Studies, Cornell University, Ithaca, New York 14853

The "direct interaction approximation" of Kraichnan as modified by Kadomtsev is employed to develop a strong turbulence theory which predicts both nonlinear frequency broadening and a power law for the spectrum of a two-dimensional convecting plasma.

In this Letter we consider well-developed strong turbulence in a low-pressure weakly ionized plasma confined in a strong magnetic field $B\hat{x}$ subjected to both a gradient in density $(\partial n/\partial z)\hat{z}$ and an electric field $\vec{E}_0 = -(\partial\varphi_0/\partial z)\hat{z}$. The electrons and ions suffer collisions predominantly with the background neutrals such that $\Omega_e \gg \nu_e$ and $\Omega_i \lesssim \nu_i$, where $\Omega_{e,i}$ and $\nu_{e,i}$ are the respective cyclotron and collisional frequencies. The difference in Ω and ν between electrons and ions gives rise to a mean current density $J\hat{y}$ resulting from the $\vec{v}_0 = \vec{E}_0 \times \vec{B}/B^2$ drift of the electrons. Simon[1] and Hoh[1] have independently shown that this configuration is unstable if $\nabla n \cdot \nabla(-e\varphi_0) > 0$, in exact analogy to the gravitational instability.[2] The unstable fluctuations have the nature of growing waves propagating in the direction of electron drift, i.e., $\varphi \sim \varphi(z)\exp[i(k_y y - \omega t)]$.

We shall be concerned here with the nonlinear development of these fluctuations leading eventually to a two-dimensional turbulent state. The model developed below applies directly to the E-region ionospheric density irregularities driven by the equatorial electrojet.[3-5] This theory predicts (i) that the power spectrum of the density fluctuations $\langle |\delta n_{\vec{k}}^+/n_0|^2\rangle \equiv I_{\vec{k}}^+$ is proportional to $|\vec{k}|^{-n}$, where n ranges at most between 3 and 4, (ii) that $I_{\vec{k}}^+$ is proportional to $|\vec{v}_0|^m$, and (iii) that the resonance broadening of the power spectrum in frequency, $\Gamma_{\vec{k}}^+$, is proportional to $k^{2-n/2}$. If we take into account that radar observations of the equatorial E-region indicate $m \simeq 2$, then this theory which relates m to n predicts $n \simeq \frac{16}{5}$, which agrees with such ionospheric data as are available and also with numerical simulations.

It appears to us that Eqs. (7) and (8) which express the mathematical content of this model could represent convective plasma motion in a broad class of experimental configurations including large toroidal machines for plasma confinement. Although the sources of the instabilities are individual to particular experiments the nonlinear interaction terms may be common to them.

Under the assumptions of quasineutrality $Zn_i \simeq n_e \equiv n$ and isothermality, the basic equations for the electron and ion (Ze) fluids are

$$\partial n/\partial t + \nabla \cdot n\vec{v}_e = 0, \qquad (1)$$

$$ne(\vec{E} + \vec{v}_e \times \vec{B}) + T_e\nabla n + nm_e\nu_e\vec{v}_e = 0, \qquad (2)$$

$$-Zn_ie(\vec{E} + \vec{v}_i \times \vec{B}) + T_i\nabla n_i + n_im_i\nu_i\vec{v}_i = 0, \qquad (3)$$

$$\nabla \cdot (\vec{J}_i + \vec{J}_e) = 0. \qquad (4)$$

On linearizing these equations about the equilibrium $n_0 = N_0(1 + z/L)$, $d\varphi_0/dz = a/(z+L)$, unstable fluctuations $\varphi = \tilde{\varphi}\exp\{i[k_y y + k_z z - (\omega_{\vec{k}r}^+ + i\gamma_{\vec{k}}^+)t]\}$, with $\vec{k}\cdot\vec{B} = 0$ and $k_y L \gg 1$, have frequency and growth rate given by[3]

$$\omega_{\vec{k}r}^+ = \vec{k}\cdot\vec{v}_0/(1+\psi), \qquad (5)$$

$$\gamma_{\vec{k}}^+ = [\psi/(1+\psi)]\{(\Omega_e/\nu_e)[k_y^2 v_0/k^2 L(1+\psi)] - k^2 C_s^2/\nu_i\}, \qquad (6)$$